Received: 12 June 2021 | Revised: 17 October 2021 | Accepted: 22 November 2021

DOI: 10.1002/cac2.12240

CANCER COMMUNICATIONS Open Access

LETTER TO THE EDITOR

Proteomics profiling of colorectal cancer progression identifies PLOD2 as a potential therapeutic target

Dear editors,

Colorectal cancer (CRC) is the second leading cause of cancer deaths in developed countries [1]. The malignant transformation from small clumps to cancer takes about 10 years [2]. This study aimed to characterize proteomic dynamics associated with CRC development and progression, and identify novel therapeutic targets for intercepting the underlying oncogenic processes. We have optimized pressure cycling technology (PCT) coupled with data-independent acquisition mass spectrometry (DIA-MS) for robust and reproducible proteomic analysis of biopsy-level formalin-fixed paraffin-embedded (FFPE) tissues [3].

In this study, we profiled the proteomic tissue landscape of CRC evolving from normal colon to hyperplastic polyps, adenomas, adenocarcinoma not otherwise specified (AC) or mucinous adenocarcinoma (MC). We identified 69,949 peptides, 6,359 protein groups, and 4,830 unique proteins (Supplementary Table S1) based on our previously established spectral library for DIA analysis [4] from 170 FFPE tissue samples (85 patients, each with 2 biological replicates) (Figure 1A). Pearson's correlation coefficient between biological replicates was 0.813, and 0.953 between technical replicates.

We identified 928 differentially expressed proteins by comparing protein expression in samples from different CRC clinical stages to normal colon tissue samples (Figure 1B). Pairwise comparisons between polyps and normal colon, adenomas and polyps, carcinoma and adenomas, as well as MC and AC revealed distinct proteomic changes associated with each transformation towards malignancy (Supplementary Figure S1A). Canonical pathways analysis revealed that the dysregulated proteins were mostly related to oxidative phosphorylation. Interestingly, oxidative phosphorylation was enhanced in precancerous tissues (hyperplastic polyps and adenomas) but suppressed in CRC tissues, suggesting metabolic adaptations of tumor cells in the evolving microenvironment (Supplementary Figure S1B). Analysis of diseases and biological functions of differential proteins in benign lesions showed proteomic perturbations associated with oncogenic pathways. For example, COPE, COPA, and COPZ1 are proteins encoded by coatomer protein complex genes which are essential proteins for tumorigenesis in CRC. PSMC3, PSMD13, PSMA7 and PSMD8 are all proteasomal proteins whose expressions began to rise in polyps and peaked in adenomas (Supplementary Figure S1C).

Six biologically significant protein expression patterns associated with CRC development were selected by unsupervised cluster analysis. Patterns 1, 2 and 3 were formed by upregulated proteins while patterns 4, 5 and 6 were formed by downregulated proteins (Figure 1C). Gene Ontology analysis for enrichment of biological processes in the six clusters (Supplementary Figure S2A) identified extracellular matrix (ECM) enrichment in pattern 3. We then checked for all ECM-related proteins in the "matrisome", which has been defined as the combination of core ECM proteins (glycoproteins, collagens, and proteoglycans) and ECM-associated proteins (ECM-affiliated proteins, ECM regulators, and secreted factors) [5]. Among the six protein expression patterns, we observed enrichment of ECM regulators in the upregulated patterns. Proteins within each pattern formed protein-protein interaction networks using Cytoscape with the GeneMania plugin (Supplementary Figure S2B).

We then narrowed our focus on proteins that were consistently upregulated along the stages of tumor progression. Among plasma membrane, nucleus, cytoplasm, extracellular space and other locations, our data showed that the cytoplasm and extracellular proteins stood out as the locations with the highest expression of dysregulated proteins (Supplementary Figure S2C). CRC progression

Abbreviations: AC, adenocarcinoma not otherwise specified; CRC, colorectal cancer; DIA-MS, data-independent acquisition mass spectrometry; ECM, extracellular matrix; FFPE, formalin-fixed paraffin-embedded; IHC, immunohistochemistry; IPA, ingenuity pathway analysis; KO, knockout; MC, mucinous carcinoma; NC, normal control; PCT, pressure cycling technology; PDXs, patient-derived xenografts; PLOD2, Procollagen-Lysine, 2-Oxoglutarate 5-Dioxygenase 2; PRM, parallel reaction monitoring; TMA, tissue microarray; WB, western blotting

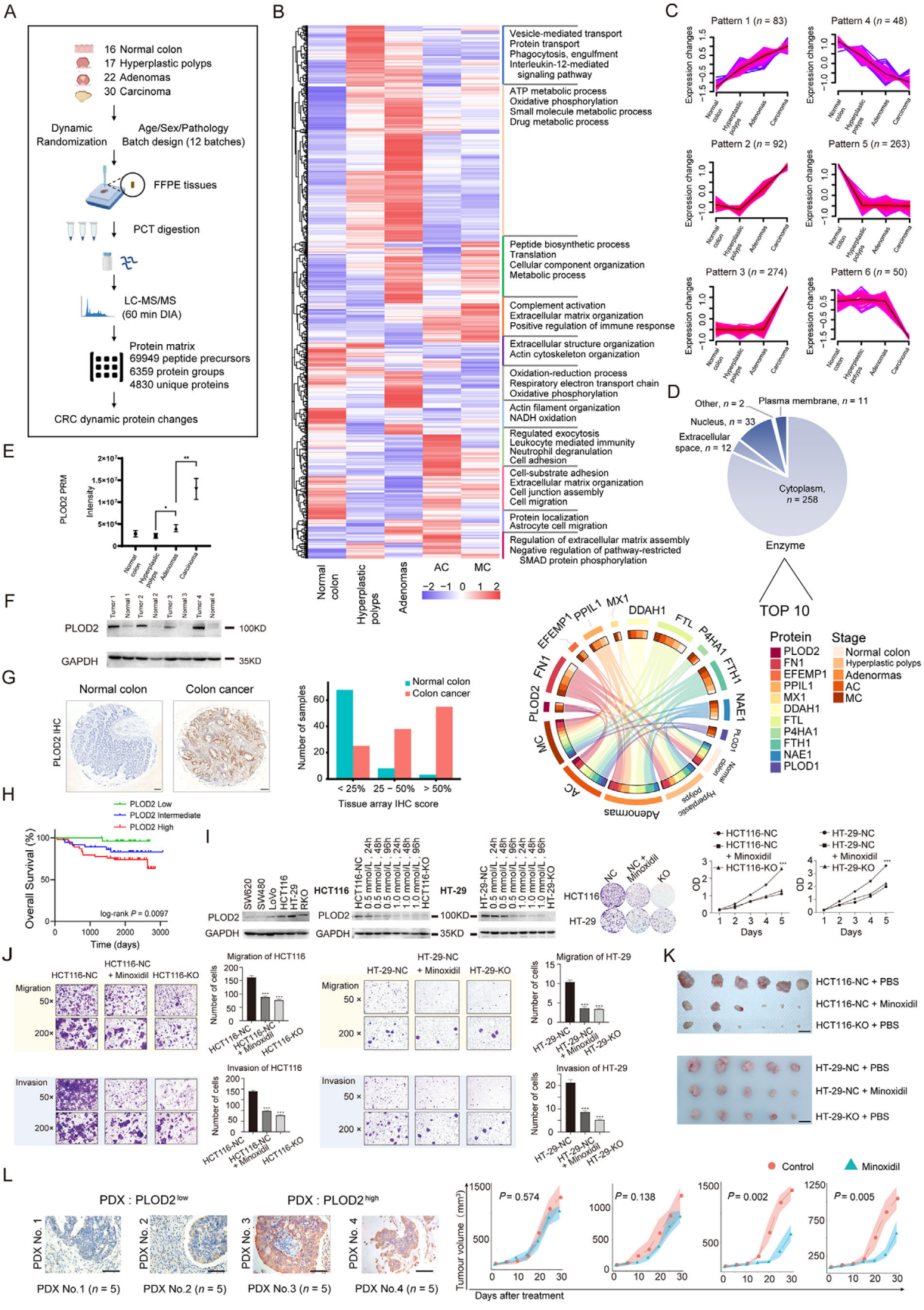
A
16 Normal colon
17 Hyperplastic polyps
22 Adenomas
30 Carcinoma
Dynamic Randomization
Age/Sex/Pathology Batch design (12 batches)
FFPE tissues
PCT digestion
LC-MS/MS (60 min DIA)
Protein matrix
69949 peptide precursors
6359 protein groups
4830 unique proteins
CRC dynamic protein changes
B
Vesicle-mediated transport
Protein transport
Phagocytosis, engulfment
Interleukin-12-mediated signaling pathway
ATP metabolic process
Oxidative phosphorylation
Small molecule metabolic process
Drug metabolic process
Peptide biosynthetic process
Translation
Cellular component organization
Metabolic process
Complement activation
Extracellular matrix organization
Positive regulation of immune response
Extracellular structure organization
Actin cytoskeleton organization
Oxidation-reduction process
Respiratory electron transport chain
Oxidative phosphorylation
Actin filament organization
NADH oxidation
Regulated exocytosis
Leukocyte mediated immunity
Neutrophil degranulation
Cell adhesion
Cell-substrate adhesion
Extracellular matrix organization
Cell junction assembly
Cell migration
Protein localization
Astrocyte cell migration
Regulation of extracellular matrix assembly
Negative regulation of pathway-restricted SMAD protein phosphorylation
Normal colon
Hyperplastic polyps
Adenomas
AC
MC
C
Pattern 1 (n = 83)
Pattern 4 (n = 48)
Pattern 2 (n = 92)
Pattern 5 (n = 263)
Pattern 3 (n = 274)
Pattern 6 (n = 50)
Expression changes
D
Other, n = 2
Plasma membrane, n = 11
Nucleus, n = 33
Extracellular space, n = 12
Cytoplasm, n = 258
Enzyme
TOP 10
E
PLOD2 PRM
Intensity
F
PLOD2
GAPDH
100KD
35KD
G
Normal colon
Colon cancer
PLOD2 IHC
Number of samples
< 25%
25 ~ 50%
> 50%
Tissue array IHC score
H
PLOD2 Low
PLOD2 Intermediate
PLOD2 High
Overall Survival (%)
log-rank P = 0.0097
Time (days)
I
SW620
SW480
LoVo
HCT116
HT-29
RKO
HCT116-NC
HCT116-KO
HT-29-NC
HT-29-KO
NC
NC + Minoxidil
KO
HCT116-NC
HCT116-NC + Minoxidil
HT-29-NC
HT-29-NC + Minoxidil
OD
Days
J
HCT116-NC
HCT116-NC + Minoxidil
HCT116-KO
HT-29-NC
HT-29-NC + Minoxidil
HT-29-KO
Migration
Invasion
Migration of HCT116
Invasion of HCT116
Migration of HT-29
Invasion of HT-29
Number of cells
K
HCT116-NC + PBS
HCT116-NC + Minoxidil
HCT116-KO + PBS
HT-29-NC + PBS
HT-29-NC + Minoxidil
HT-29-KO + PBS
L
PDX : PLOD2low
PDX : PLOD2high
PDX No. 1
PDX No. 2
PDX No. 3
PDX No. 4
PDX No.1 (n = 5)
PDX No.2 (n = 5)
PDX No.3 (n = 5)
PDX No.4 (n = 5)
Control
Minoxidil
P = 0.574
P = 0.138
P = 0.002
P = 0.005
Tumour volume (mm³)
Days after treatment
Protein
PLOD2
FN1
EFEMP1
PPIL1
MX1
DDAH1
FTL
P4HA1
FTH1
NAE1
PLOD1
Stage
Normal colon
Hyperplastic polyps
Adenomas
AC
MC

was associated with substantially increased expression of multiple enzymes (Supplementary Figure S3A). Of note, Procollagen-Lysine, 2-Oxoglutarate 5-Dioxygenase 2 (PLOD2) was the most up-regulated protein (Figure 1D and Supplementary Figure S3B). We further performed a pairwise comparison between pre-cancerous and cancerous samples with benign samples, and PLOD2 consistently outstood as the top hit (Supplementary Figure S3C).

Next, we randomly selected eight samples of each tissue type (normal colon, hyperplastic polyps, adenomas, AC, and MC) for targeted measurement of PLOD2 using parallel reaction monitoring (PRM). The PRM data from the 40 samples confirmed the elevation of PLOD2 (Figure 1E). As further verification, western blot (WB) analysis was performed on four new CRC patients and observed higher PLOD2 expression in CRC tissues than in matched para-tumoral normal colon (Figure 1F). We also assessed PLOD2 expression by immunohistochemistry staining (IHC) of tissue microarrays (TMAs) containing 118 CRC (8^{th} AJCC TNM Stage II) and 79 para-tumoral normal colon tissues (Supplementary Table S2). The IHC staining of PLOD2 in para-tumoral normal colon tissues showed that 68 samples had < 25% positive colon cells, eight samples had 25%-50%, and only three samples had > 50%. In contrast, CRC tissues showed significantly higher PLOD2 expression than para-tumoral normal colon (Figure 1G). Remarkably, we found that higher PLOD2 expression was associated with poorer overall survival of CRC patients (Figure 1H, Supplementary Table S2).

Next, we measured the PLOD2 expression in six CRC cell lines and chose the two with the highest PLOD2 expression, namely HCT116 and HT-29, for generating PLOD2-knockout (KO) congener lines using CRISPR-Cas9. Each congenic pair of cell lines was treated with increasing concentrations of minoxidil, a lysyl hydroxylase inhibitor of PLOD2. Minoxidil inhibited PLOD2 expression in both wild-type cell lines in a time- and dose-dependent manner, while clonogenicity and cell proliferation were dramatically suppressed when PLOD2 was inhibited by minoxidil or knocked-out (Figure 1I). In addition, both minoxidil treatment and PLOD2-KO suppressed CRC cell migration and invasion (Figure 1J).

Extending our findings to in vivo model, we injected HCT116 and HT-29 cell lines subcutaneously into nude mice. We tested the effects of placebo versus minoxidil treatment in vivo on tumors generated by wild-type HCT116 and HT-29 cells, and also compared the growth of tumors generated by PLOD2-KO HCT116 and HT-29 cells with PLOD2-high tumors. Our data showed that both minoxidil and CRISPR-Cas9-mediated PLOD2 suppression led to a significant decrease in tumor volume (Figure 1K). A second in vivo model was patient-derived xenografts (PDX) tumors from four CRC patients. Patient tumors with high PLOD2 levels (PLOD2 positive tumor cells were > 80%) were sensitive to minoxidil inhibition while PLOD2-negative tumors were resistant (Figure 1L), highlighting the potential clinical application of targeted therapy against PLOD2.

To gain mechanistic insight on how PLOD2 inhibition suppresses CRC tumors, we compared the transcriptome and proteome of HCT116-KO and the HCT116-normal control (NC) cell lines using RNA sequencing and DIA-MS,

FIGURE 1 Proteomics profiling of colorectal cancer progression and validation of PLOD2 as a potential therapeutic target. (A) Schematic diagram of the experimental design of this study. (B) Summary heatmap of expression of all dysregulated proteins in each group (hyperplastic polyps, adenomas, adenocarcinoma not otherwise specified and mucinous adenocarcinoma compared with the normal colon group, and enriched functional pathways of the differentially expressed proteins. (C) Unsupervised clustering of proteome dynamics revealed six protein patterns in CRC progression. Each line indicates the relative abundance of each protein and is color-coded by cluster membership. "*n*" denotes the number of proteins per cluster. (D) Protein localization statistics of dysregulated enzymes in CRC compared with the normal colon group showing differential PLOD2 expression to be the most significant. (E) Expression of PLOD2 by PRM-MS. Data are mean ± SEM, *: $P < 0.05$, **: $P < 0.01$. (F) Western blot of PLOD2 in CRC tumor and paired normal colon tissue of four new patients. (G) Representative IHC stained PLOD2 expression in CRC and normal colon tissues from TMA and the corresponding percent of PLOD2 positive colon or tumor cells. Scale bar represents 100 μm. (H) Kaplan–Meier curves of overall survival (OS) of CRC patients based on TMA PLOD2 expression scores (low, $n = 27$; Intermediate, $n = 37$ and high, $n = 54$, $P = 0.0097$, two-sided log-rank test. (I) Western blot analysis of PLOD2 in CRC cell lines (SW620, SW480, LoVo, HCT116, HT-29, RKO). WB of PLOD2 in HT-29, HCT116, their congenic knockout derivative cell lines, and minoxidil-treated groups with different concentrations (0.5 mmol/L, 1 mmol/L) or duration (24h, 48h, 96h). Colony formation and cell proliferation assays for HT-29, HCT116, their KO cell lines and 1 mmol/L minoxidil-treated groups ($n = 3$ biological replicates). (J) Cell migration and invasion assays of HT-29, HCT116, their KO cell lines and 1 mmol/L minoxidil-treated groups ($n = 3$ biologically independent experiments). (Left panel, representative images of transwell chambers, 50 × and 200 ×; right panel, average counts of five random microscopic fields at a magnification of 200 × . Data are mean ± SEM, ***: $P < 0.001$). (K) Subcutaneous mouse models and corresponding dissected subcutaneous tumors. For both HT-29 and HCT116, three groups (-NC + PBS, -NC + minoxidil and -KO + PBS) were intraperitoneally injected every other day for a total of 10 injections ($n = 5$~6 mice per group). Scale bar represents 1 cm. (L) Growth curves of PDX models treated by minoxidil on the indicated days ($n = 5$ mice per group). Circles and triangles denote the mean volume of tumors (mean ± SEM). Immunohistochemical staining of PLOD2 in PDX tumors is labeled on the top. Scale bar represents 100 μm. *P*-values were calculated using the two-tailed Student's *t*-test. NS, not significant

respectively (Supplementary Table S3). We identified 1236 up- and 955 down-regulated transcripts, and 227 up- and 127 down-regulated proteins (Supplementary Figure S4A). The data indicated that PLOD2 contributed to tumor growth, resistance to cell necrosis, and was closely related to the development of colorectal cancer (Supplementary Figure S4B). PLOD2 was also involved in protein synthesis, metabolism, and mRNA translation (Supplementary Figure S4C). Selected protein networks prioritized by these analyses are shown in Supplementary Figure S4D and E. An overview of the patients' basic pathological characteristics is shown in Supplementary Table S4.

Compared to previous studies [6, 7], our study systematically tracked a plethora of protein changes in CRC tissues as the disease progressed through increasing degrees of malignancy. Therapeutic interventions directed at cancer-derived ECM and their regulatory factors may be clinically effective [8]. PLOD family proteins catalyze post-translational modifications of collagen by converting lysine to hydroxylysine, which promotes stable interactions and deposition of collagen [9]. PLOD2 could be induced in L1CAM-overexpressing CRC cell lines and promoted L1CAM-mediated CRC progression by inducing ezrin signaling and the SMAD2/3 pathway [10]. Our data collectively constitute plausible evidence for suggesting further research on PLOD2 as a promising therapeutic target in CRC tumors in the emerging practice of precision oncology.

DECLARATIONS

ETHICS APPROVAL AND CONSENT TO PARTICIPATE

Written informed consent was obtained from all participants based on the guidelines of the Declaration of Helsinki. Human tissue samples were collected with the approval of the Institutional Ethics Committee of the Second Affiliated Hospital of Zhejiang University, School of Medicine (Zhejiang, P. R. China, No.2020-322). Animal studies and formalin-fixed paraffin-embedded samples collections were approved by the Institutional Ethics Committee of the Second Affiliated Hospital Zhejiang University School of Medicine (SYXK2018-0012).

CONSENT FOR PUBLICATION

All authors read and approved the final manuscript for publication.

AVAILABILITY OF DATA AND MATERIAL

The MS proteomics data are available on the iProX database with the project ID: IPX0001414000 and the subproject ID: IPX000141400. The raw sequence data have been uploaded to SRA with an ID: PRJNA598559.

COMPETING INTERESTS

The authors declare that they have no competing interests.

FUNDING

This work was supported by the National Key Research and Development Program of China (Grant No. 2017YFC0908200), National Natural Science Foundation of China (Grant No. 81972270, 81972492, 32027801, 21904107), the Zhejiang Provincial Science Foundation for Distinguished Young Scholars (Grant No. LR19C050001), Hangzhou Agriculture and Society Advancement Program (Grant No. 20190101A04) and 2019 Zhejiang University Academic Award for Outstanding Doctoral Candidates to YK.S (Grant No. 2019071).

AUTHORS' CONTRIBUTIONS

YKS, KLX, XZ, BTZ, XLZ, LW, YTS, DL performed experiments and data interpretation. TC, JW, SJY, LFS, XMX, LNQ, JNC, WXH, XYW, XPX, JFL, LRC, JMS, SZ provided key biological samples and materials. YKS, KLX, LW, DL, SZD, HHG, GR, YTS, WL, XC, TSZ, YZ, ZYH, TNG performed data analysis. YKS, KLX, XZ, BTZ, YTS, SZ, JMS, TNG designed the study, interpreted the data, and wrote the manuscript. All authors read and approved the final manuscript.

ACKNOWLEDGMENTS

We particularly acknowledge the Biobank of the Second Affiliated Hospital of Zhejiang University School of Medicine. We thank Westlake University Supercomputer Center for assistance in data storage and computation and the Biomedical Core facility for mass spectrometry analysis. We thank Prof. Yongzhan Nie (Air Force Medical University) for his guidance in writing. We thank Dr. Oi Lian Kon for editing the manuscript.

Yingkuan Shao[1,2,3]
Kailun Xu[1,2,3]
Xi Zheng[1,2,3]
Biting Zhou[1]
Xiuli Zhang[4]
Lin Wang[5]
Yaoting Sun[2,3]
Dan Li[1]
Ting Chen[1]
Jian Wang[6]
Shaojun Yu[6]
Lifeng Sun[6]
Xiaoming Xu[7]
Shaozhi Dai[2,3]
Huanhuan Gao[2,3]
Guan Ruan[2,3]
Wei Liu[2,3]

Xue Cai[2,3]
Tiansheng Zhu[2,3]
Lina Qi[1]
Jiani Chen[1]
Wangxiong Hu[1]
Xingyue Weng[1]
Yi Zhu[2,3]
Xueping Xiang[7]
Zhiyuan Hu[4,8,9]
Jinfan Li[7]
Lirong Chen[7]
Jimin Shao[1,10]
Shu Zheng[1]
Tiannan Guo[2,3]

[1] *Key Laboratory of Cancer Prevention and Intervention, Ministry of Education, Department of Breast Surgery and Oncology, Second Affiliated Hospital, School of Medicine, Cancer InstituteZhejiang University, Hangzhou, Zhejiang 310009, P. R. China*
[2] *Zhejiang Provincial Laboratory of Life Sciences and Biomedicine, Key Laboratory of Structural Biology of Zhejiang Province, School of Life Sciences, Westlake University, 18 Shilongshan Road, Hangzhou, Zhejiang 310024, P. R. China*
[3] *Institute of Basic Medical Sciences, Westlake Institute for Advanced Study, 18 Shilongshan Road, Hangzhou, Zhejiang 310024, P. R. China*
[4] *CAS Key Laboratory of Standardization and Measurement for Nanotechnology, CAS Key Laboratory for Biomedical Effects of Nanomaterials and Nanosafety, CAS Center for Excellence in Nanoscience, National Center for Nanoscience and Technology of China, Beijing 100190, P. R. China*
[5] *Zhejiang Provincial Key Laboratory of Pancreatic Disease, The First Affiliated Hospital, Zhejiang University School of Medicine, Hangzhou, Zhejiang, P. R. China*
[6] *Department of Colorectal Surgery, the Second Affiliated Hospital of Zhejiang University School of Medicine, Hangzhou, Zhejiang 310009, P. R. China*
[7] *Department of Pathology, The Second Affiliated Hospital, Zhejiang University School of Medicine, Hangzhou, Zhejiang 310009, P. R. China*
[8] *School of Nanoscience and Technology, Sino-Danish College, University of Chinese Academy of Sciences, Beijing 100049, P. R. China*
[9] *Fujian Provincial Key Laboratory of Brain Aging and Neurodegenerative Diseases, School of Basic Medical Sciences, Fujian Medical University, Fuzhou, Fujian 350108, P. R. China*
[10] *Department of Pathology and Pathophysiology, Key Laboratory of Disease Proteomics of Zhejiang Province, Zhejiang University School of Medicine, Hangzhou, Zhejiang 310058, P. R. China*

Correspondence
Jimin Shao and Shu Zheng, Cancer Institute, Key Laboratory of Cancer Prevention and Intervention, Ministry of Education, Department of Breast Surgery and Oncology, Second Affiliated Hospital, School of Medicine, Zhejiang University, Hangzhou 310009, Zhejiang, P. R. China.
Email: shaojimin@zju.edu.cn; zhengshu@zju.edu.cn
Tiannan Guo, Zhejiang Provincial Laboratory of Life Sciences and Biomedicine, Key Laboratory of Structural Biology of Zhejiang Province, School of Life Sciences, Westlake University, 18 Shilongshan Road, Hangzhou 310024, Zhejiang, P. R. China.
Email: guotiannan@westlake.edu.cn

Yingkuan Shao and Kailun Xu contributed equally to this work.

ORCID
Yingkuan Shao https://orcid.org/0000-0001-9683-5691
Kailun Xu https://orcid.org/0000-0002-8458-3551
Jimin Shao https://orcid.org/0000-0003-4792-5433
Shu Zheng https://orcid.org/0000-0002-2521-190X
Tiannan Guo https://orcid.org/0000-0003-3869-7651

REFERENCES

1. Siegel RL, Miller KD, Fuchs HE, Jemal A. Cancer Statistics, 2021. CA Cancer J Clin. 2021;71(1):7-33.
2. Jemal A, Bray F, Center MM, Ferlay J, Ward E, Forman D. Global cancer statistics. CA: A Cancer Journal for Clinicians. 2011;61(2):69-90.
3. Zhu Y, Weiss T, Zhang Q, Sun R, Wang B, Yi X, et al. High-throughput proteomic analysis of FFPE tissue samples facilitates tumor stratification. Mol Oncol. 2019;13(11):2305-28.
4. Zhu T, Zhu Y, Xuan Y, Gao H, Cai X, Piersma SR, et al. DPHL: A DIA Pan-human Protein Mass Spectrometry Library for Robust Biomarker Discovery. Genomics Proteomics Bioinformatics. 2020;18(2):104-19.
5. Naba A, Clauser KR, Hoersch S, Liu H, Carr SA, Hynes RO. The Matrisome: In Silico Definition and In Vivo Characterization by Proteomics of Normal and Tumor Extracellular Matrices. Molecular & Cellular Proteomics. 2012;11(4):M111.014647. http://doi.org/10.1074/mcp.m111.014647
6. Wiśniewski JR, Duś-Szachniewicz K, Ostasiewicz P, Ziółkowski P, Rakus D, Mann M. Absolute Proteome Analysis of Colorectal Mucosa, Adenoma, and Cancer Reveals Drastic Changes in Fatty Acid Metabolism and Plasma Membrane Transporters. J Proteome Res. 2015;14(9):4005-18.
7. Mu Y, Chen Y, Zhang G, Zhan X, Li Y, Liu T, et al. Identification of stromal differentially expressed proteins in the colon carcinoma by quantitative proteomics. Electrophoresis. 2013;34(11):1679-92.

8. Tian C, Clauser KR, Ohlund D, Rickelt S, Huang Y, Gupta M, et al. Proteomic analyses of ECM during pancreatic ductal adenocarcinoma progression reveal different contributions by tumor and stromal cells. Proc Natl Acad Sci USA. 2019;116(39):19609-18.
9. Qi Y, Xu R. Roles of PLODs in Collagen Synthesis and Cancer Progression. Front Cell Dev Biol. 2018;6:66.
10. Cheriyamundath S, Kumar A, Gavert N, Brabletz T, Ben-Ze'ev A. The Collagen-Modifying Enzyme PLOD2 Is Induced and Required during L1-Mediated Colon Cancer Progression. Int J Mol Sci. 2021;22(7):3552.

SUPPORTING INFORMATION

Additional supporting information may be found in the online version of the article at the publisher's website.